

## **Peculiarities of mesosphere/lower thermosphere parameters during solar minimum 23/24**

**Ch. Jacobi<sup>1</sup>, P. Hoffmann<sup>1</sup>, C. Unglaub<sup>1</sup>, M. Placke<sup>2</sup>, G. Stober<sup>2</sup>**

<sup>1</sup>Institute for Meteorology, University of Leipzig, Stephanstr. 3, 04103 Leipzig, Germany

<sup>2</sup>Leibniz Institute of Atmospheric Physics at the Rostock University, Schloßstraße 6, 18225 Kühlungsborn, Germany

### **Abstract**

The 2009 solar minimum 23/24 has been characterized by an anomalous strong decrease in thermospheric density. We analyze anomalies of mesosphere/lower thermosphere parameters possibly connected with this effect. Nighttime mean low-frequency reflection heights measured at Collm, Germany, show a very strong decrease after 2005, indicating a density decrease. This decrease is also visible in mean meteor heights measured with a VHF meteor radar at Collm. It is accompanied by an increase/decrease of gravity wave (GW) amplitudes in the upper mesosphere/lower thermosphere. On the decadal scale, GWs are negatively correlated with the background zonal wind, but this correlation is modulated in the course of the solar cycle, indicating the combined effect of GW filtering and density decrease.

### **Zusammenfassung**

Das solare Minimum des Jahres 2009 war durch außerordentlich starken Rückgang thermosphärischer Dichte charakterisiert. Hier werden Parameter der Mesosphäre und unteren Thermosphäre untersucht, deren Variabilität eventuell mit diesem Effekt zusammenhängt. Im Einzelnen war ein starker Rückgang der Reflexionshöhe von Langwellen zu verzeichnen, der sich auch in Meteorhöhen zeigt. Dieser Rückgang, verursacht durch geringere Dichte, war mit einer Zunahme/Abnahme atmosphärischer Schwerewellen in der Mesosphäre/unteren Thermosphäre verbunden. Atmosphärische Schwerewellen in der Mesosphäre werden durch den Grundwind gesteuert; der Zusammenhang variiert jedoch im Verlauf des Sonnenfleckenzyklus.

### **1 Introduction**

It is widely known that solar variability influences the atmosphere (e.g., Gray et al., 2010), e.g. the dynamics of the middle and upper atmosphere. In particular, search for an effect of the 11-year solar Schwabe cycle has been undertaken, for example, to partly explain the observed variability of the mesosphere and lower thermosphere (MLT), which can be studied, e.g., by radars. Indeed, indication for a solar effect has been found in MLT radar wind time series over Central Europe (Jacobi and Kürschner, 2006; Keuer et al., 2007).

Solar cycles are different from one to another. Especially, the recent solar minimum 23/24 has been extremely extended and extraordinarily deep. Consequently, it led to extreme upper atmosphere reactions, in particular a decrease in thermospheric

density (Emmert et al., 2010; Solomon et al., 2010) which exceeds the expectations that would have been based on conventional solar indices like the sunspot number or the F10.7 radio flux.

Lower ionospheric electron density reacts on solar extreme ultraviolet (EUV) variations, which leads to a quasi 11-year modulation of radio wave reflection heights. These have been observed, e.g., by Kürschner and Jacobi (2003) who found that low-frequency (LF) radio wave ionospheric reflection heights measured at Collm (177 kHz, distance to transmitter about 160 km) are about 2 km lower during solar maximum than during solar minimum. This is owing to the increased ionisation during solar maximum, however, this effect is superposed by thermal shrinking of the mesosphere during solar minimum, since the middle atmosphere has a solar cycle signal of about 2 K difference between maximum and minimum. However, this thermal shrinking is usually overcompensated by increased ionisation. We are interested, whether the recent extreme solar minimum has led to anomalous signatures either in MLT wind or density. We focus on the summer MLT, which is not that much influenced by stratospheric planetary wave activity.

## 2 Measurements

### 2.1 Collm LF lower ionospheric drifts, reflection heights, and GW estimates

At Collm Observatory (51.3°N, 13°E), MLT winds have been obtained by D1 LF radio wind measurements from 1959-2008, using the sky wave of three commercial radio transmitters. The data are combined to half-hourly zonal ( $u$ ) and meridional ( $v$ ) mean wind values. The virtual reflection heights have been estimated since late 1982 using measured travel time differences between the separately received sky wave and the ground wave (Kürschner et al., 1987) of one transmitter (Zehlendorf near Berlin, frequency 177 kHz, reflection point at 52.1°N, 13.2°E). More details of the Collm LF system are given in Jacobi (2011).

Since the LF reference height changes in the course of the day, a continuous time series is not available and consequently GW spectra cannot be calculated. However, using the method presented by Gavrilov et al. (2001), horizontal wind fluctuations  $u'$  and  $v'$  in the period range 0.7-3 h can be estimated from the wind measurements on 177 kHz, which may be taken as GW proxy. Jacobi et al. (2006) has used this method to analyze Collm wind fluctuations from 1984–2003. They found an 11-year solar cycle with larger GW amplitudes during solar maximum, but their dataset did not include the recent solar minimum.

### 2.2 Collm meteor radar

A SKiYMET meteor radar (MR) is operated at Collm Observatory on 36.2 MHz to measure horizontal winds, meteor rates and heights (height range approx. 80-100 km), and further meteor parameters since August 2004. The radar and the hourly wind detection are described in Jacobi (2011). Monthly mean wind parameters are obtained from half-hourly mean winds applying a multiple regression analysis including the mean wind, and tidal components. Based upon 2-hourly means, GW variances and

fluxes are obtained by fitting the 2-hourly mean GW fluxes to the radial drift variances according to Hocking (2005). Details can be found in Placke et al. (2010).

### 2.3 GW potential energy from TIMED/SABER temperature profiles

The SABER instrument onboard the TIMED satellite (Russell et al., 1999; Mertens et al., 2001) scans the atmosphere from about  $52^\circ$  on one hemisphere to  $83^\circ$  on the other one. This latitude range is reversed by a yaw manoeuvre every 60-days. Due to the sun-synchronous orbital geometry the spacecraft passes the equator always at the same local time (12LT) on the day side. Each single temperature profile, having a vertical resolution of 0.5 km, is high-pass filtered to analyze waves with vertical wavelength of up to 6 km. From these filtered data, the vertical structure of GW amplitudes and their specific potential energy is obtained. This method has frequently been applied to GPS radio occultations (e.g., Fröhlich et al., 2007). The total energy integrated over a sliding vertical column (10 km) is used to study GWs. Note that limb scanning of the atmosphere as is made by SABER only reveals certain parts of the GW spectrum due to the integration along the line of sight (Preusse et al., 2006). Another limitation is made by the chosen vertical filter, which allows only GWs of short wavelengths to be studied.

## 3 GW proxy decadal variability

Jacobi et al. (2006) had shown that there is a solar cycle influence on GW activity as measured by LF over Collm. Figure 1 presents the summer (JJA) mean time series of GW variance  $\zeta^2 = u'^2 + v'^2$  at 100 km virtual height, which represents approximately 91 km real height (Jacobi, 2011). The data are an update from Jacobi et al. (2006). The so-called 13-monthly mean (which is actually a 12-monthly mean but centered at the respective month) sunspot number is added. Clearly, there is a solar cycle in the GW variance, and from visual inspection a decreasing long-term trend is also visible. We thus added, as a red solid line, a least squares fit of a linear trend  $b$  (intercept  $a$ ) superposed by a solar cycle (coefficient  $c$ )

$$\zeta^2 = a + b \cdot t + c \cdot R, \quad (1)$$

with  $t$  as the time in years and  $R$  as the 13-monthly mean relative sunspot number. We are only interested in long-term and qualitative connections, so employing other widely used solar proxies as F10.7 are not superior to use of  $R$  here. As can be seen in the lower part of the figure, the residuals are not normally distributed, and generally the model is not valid during the 1996 as well as the recent solar minimum. Using the same model, but including only data until 1995 (blue line) reveals that the time interval until the early 2000s is well represented by that model, and after 2004 there is a drastic change. We therefore conclude that there is a change in dynamical regime since about 2004.

In the case of saturated GWs, linear theory predicts amplitudes proportional to the intrinsic phase speed. Consequently, since GW phase speeds must be positive (eastward) in the summer MLT owing to the filtering effect of the stratospheric and mesospheric easterlies, a negative correlation is expected between the background wind and the GW amplitudes. In Figure 2 we present GW variance together with the

background mean zonal wind at 100 km virtual height. Note that the background wind is simply the mean of the zonal wind averaged over those times when GW amplitudes have been calculated, and thus may deviate from the prevailing wind. There is an overall anticorrelation between GW variances and zonal winds, as expected from linear theory.

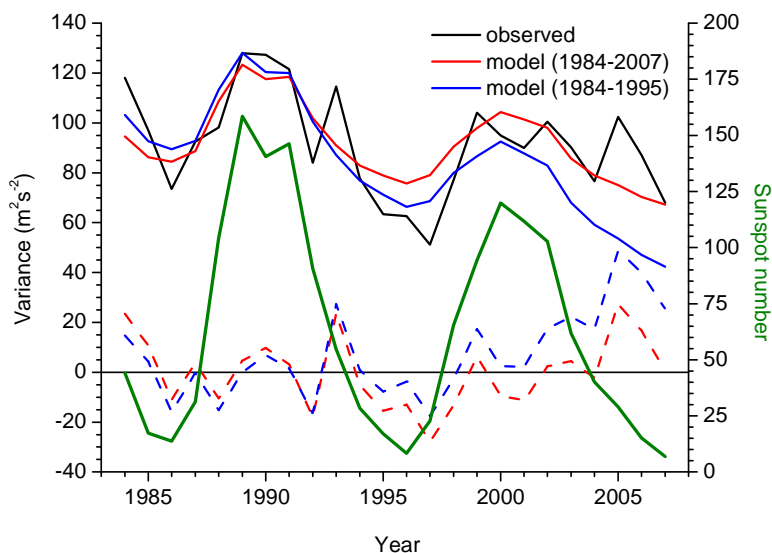


Figure 1: JJA mean LF GW proxy, and fit including linear trend and a solar cycle according to Eq. (1) at 100 km virtual height (approx. 91 km real height). The fit was performed both using the complete dataset 1984-2007 (red curve) and using part of the dataset until 1995 (blue curve). In the lower part the respective residuals are given as dashed lines. The sunspot number is also added as green line.

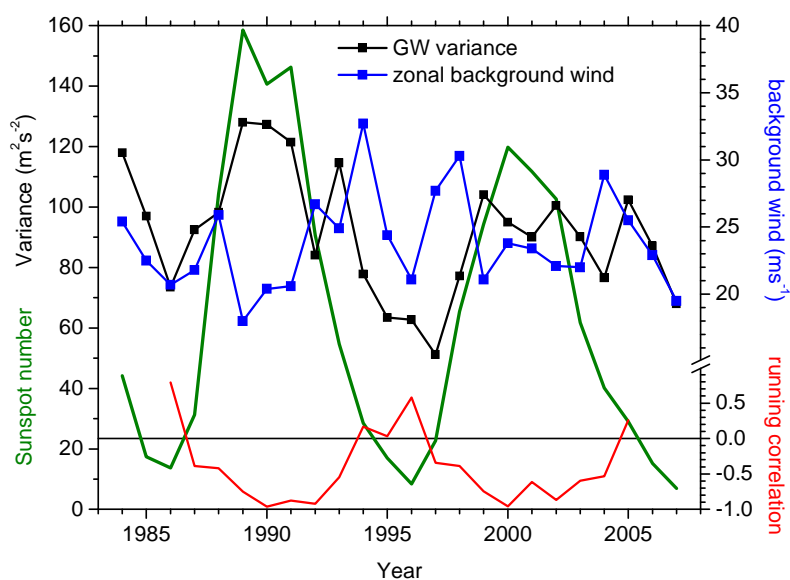


Figure 2: JJA mean LF GW proxy (black) and zonal mean wind (blue) at 100 km virtual height. In the lower part of the figure, running correlation coefficients between GW proxy and mean wind are added. The sunspot number is added as green line.

However, during solar minimum the correlation reverses. The running correlation (Kodera, 1993) between GW proxy and mean zonal wind is added in the lower part of Figure 2. Due to the shortness of the time series, only 5 data points are used for each calculation. A clear solar cycle modulation is visible. The running correlation time series is modulated by the sunspot number cycle with a correlation coefficient of  $r = -0.80$ . It is also remarkable that this modulation takes place during each solar minimum since 1986. Note also that that GW variances increase in 2005, when solar flux already decreases and thus decreasing GW variances are expected. This pattern has its counterpart in a GW variance peak in 1993. We may conclude that there is obviously a different regime of mean wind-GW coupling during solar minimum, which is, however, more emphasized during the recent minimum.

LF height measurements at Collm have been terminated after 2007, so that the solar minimum is not covered by them. To analyze winds and waves during the minimum, in Figure 3 MR summer mean zonal prevailing winds at 6 height gates are presented. Clearly, interannual variability of winds in the upper and lower height gates is opposite. This is explained by GW acceleration and filtering in the mesosphere. In the case of strong/weak mesospheric easterlies, GW amplitudes are large/small, which then lead to strong/weak vertical wind shear. Figure 3 also shows that above 91 km winds are decreasing until 2007, which is qualitatively consistent with the decrease of the LF winds during 2005-2007. After 2007, winds are increasing again. This agrees with the zonal LF wind decrease after 1994 (Figure 2). This zonal wind decrease is accompanied by GW proxy amplitude decrease. MR GW analyses of the recent minimum (Figure 4) again show this effect qualitatively. The same is the case for SABER potential energy (Figure 5), although here only the GW amplitudes above  $\sim 100$  km decrease with time. This may be due to the fact that we present zonal mean potential energy, while Figures 1-4 represent point measurements and non-zonal structures are likely to exist in the MLT. Note that the above mentioned trends are only valid for heights above 90 km, while for the lower height gates the winds and GW amplitudes behave in an opposite manner.

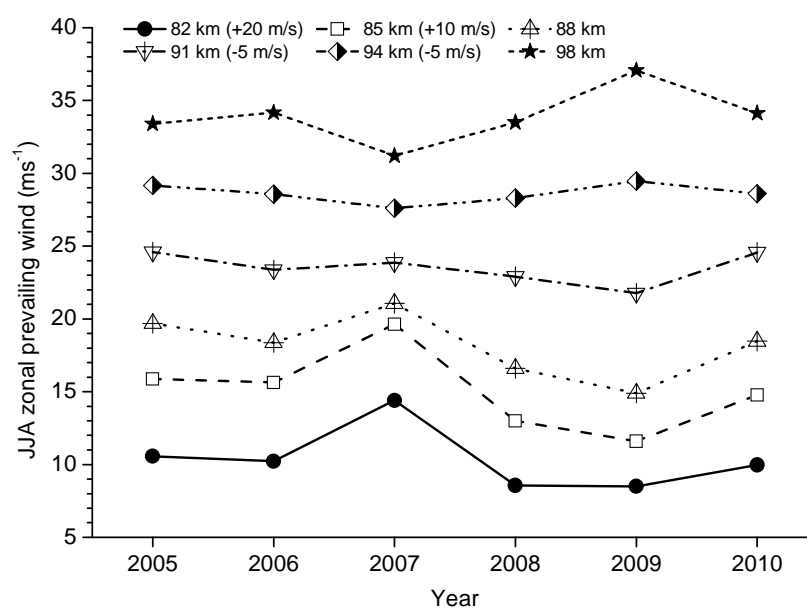


Figure 3: Collm June-August mean zonal prevailing winds measured by meteor radar.

## 5 LF virtual heights and mean meteor altitudes

The solar modulation of correlation between zonal wind and GW amplitudes suggests that the decrease of reference height of wind systems may play a role. Collm LF virtual nighttime (22-2LT) reflection heights are shown in Figure 6. A multiple linear fit after Eq. (1), but analyzing virtual height instead of variance is added as red line, as well as the residuals (red dashed line). The sunspot number is added as green line. Note that real heights and height differences are much smaller than virtual height differences. Thus, the strong decrease of LF heights after 2005, for example, represents a real height decrease of 2 km only. From the residuals in Figure 6 one can see that the recent minimum is outstanding. Generally, there is an ionization driven solar cycle of reflection heights such that these are lower during solar maximum than during solar minimum. Thus, the strong decrease after 2005 is unexpected. However, a similar variability has already been observed after 1993 during the last solar minimum, although with much smaller amplitudes, LF reflection height variability is influenced by changes in ionization and mesospheric shrinking. According to Figure 6 this would mean that during the recent solar minimum thermal shrinking has overcompensated the ionization effect.

Note that the LF reference height changes shown in Figure 6 do not correspond to the variations of a line of constant pressure or density. A better proxy is the mean height of meteors because these, constant meteor parameters as mean mass and velocity assumed, burn at a height that is determined by the density distribution. Figure 7 shows June-August mean meteor heights from 2005-2010, plotted against the so-called EUV-TEC index (Unglaub et al., 2011), which essentially describes the variability of the normalized solar EUV flux and is based on TIMED-SEE (Woods et al., 2000, 2005) satellite measurements. As expected, the meteor heights increase with solar activity. Note, however, that the mean meteor heights during 2008 and 2010, at the same level of solar EUV flux, are different. This is partly due to the fact that the decrease is

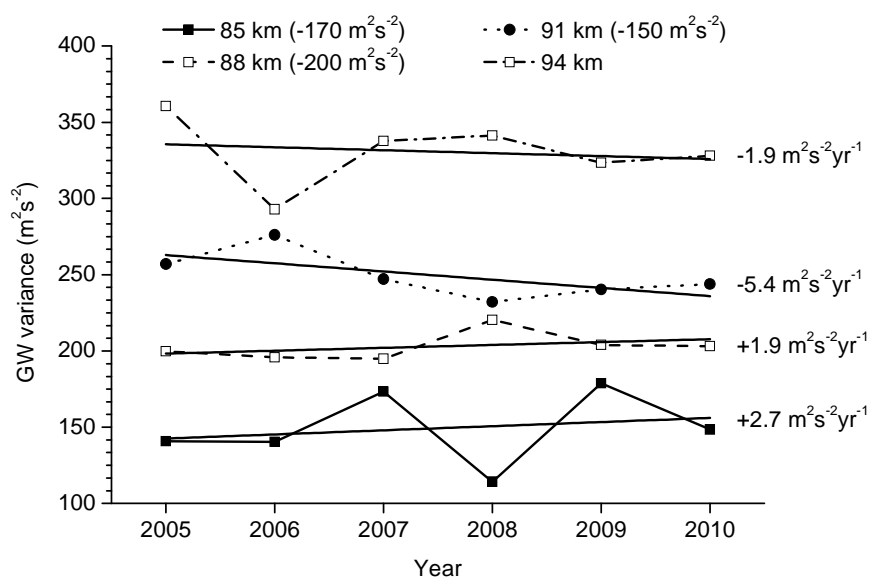


Figure 4: Horizontal wind variance calculated within 2-hr intervals using Collm MR horizontal wind measurements for 4 height gates.

superposed by the long-term changes of mesospheric density. Bremer and Peters (2008) found a long-term decrease of -30 m/yr from LF reflection heights (and excluding the solar cycle). Subtracting this from the measured meteor heights in Figure 7 (red line) shows that then the 2008 and 2010 heights, at the same solar EUV flux, have exactly the same values when long-term cooling of the middle atmosphere is taken into account.

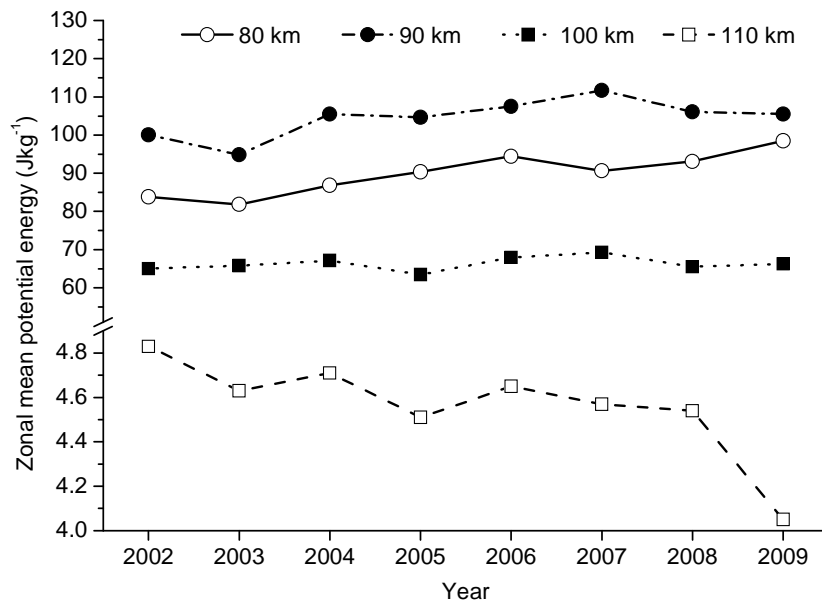


Figure 5: JJA mean potential energy at 45°N from SABER temperature profiles. Data are averages over a 10 km vertical window, and means over all longitudes.

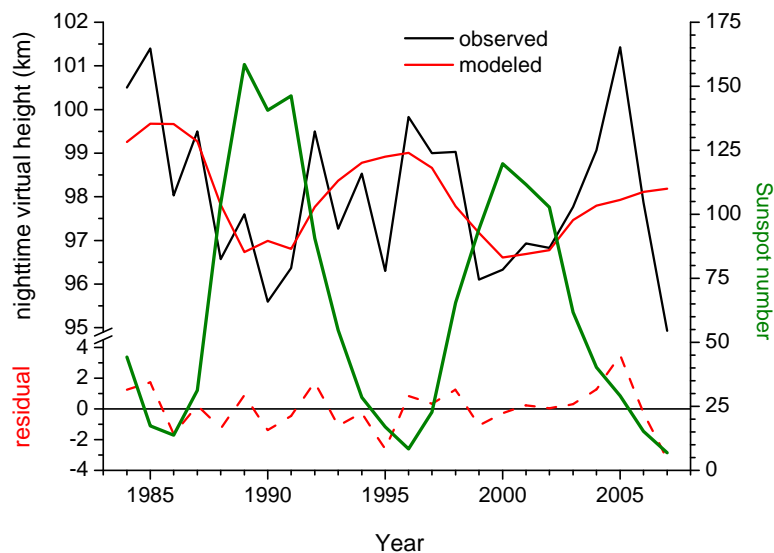


Figure 6: Collm LF virtual nighttime (22-2LT) reflection heights. A linear fit according to Eq. (1) is added as red line, as well as the residuals (red dashed line). The sunspot number is added as green line.

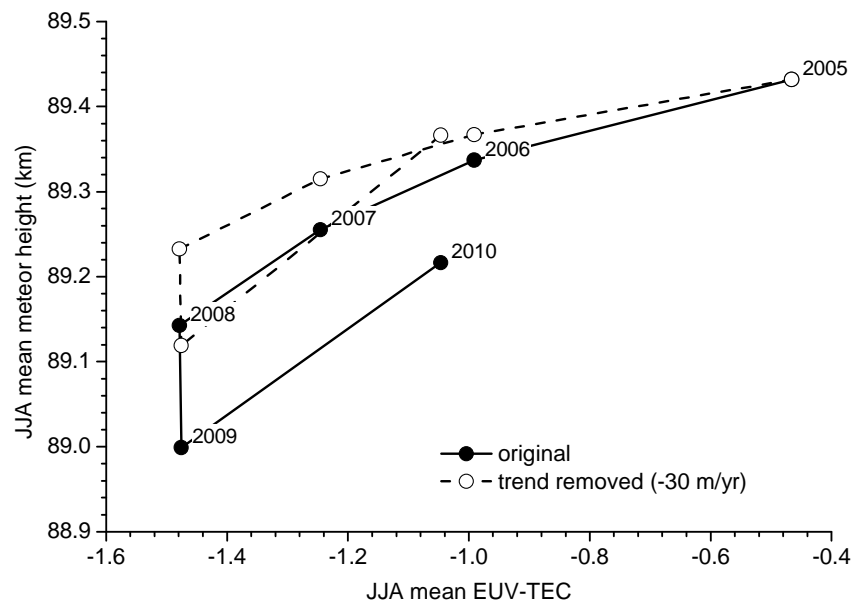


Figure 7: JJA mean meteor heights over Collm vs. EUV-TEC Index. The dashed curve represents meteor heights after removing a linear trend of  $-30$  m/yr.

There remains some hysteresis, so that the density recovers one year later than the solar EUV does. A delay of one year of noctilucent cloud occurrence and solar activity has been reported by DeLand et al. (2006) and Bremer et al. (2009). Ortiz de Adler and Elias (2008) showed a similar hysteresis in ionospheric foF2 data. Jacobi et al. (2008) showed that MLT planetary wave activity lags the solar cycle by 1-3 years.

## 6 Discussion and conclusions

Linear theory predicts that GW amplitudes are proportional to the intrinsic phase speed and thus, in the case of a given GW with specified phase speed, determined by the zonal wind itself. Since only GWs with positive phase speeds propagate to the MLT, stronger/weaker mean winds mean smaller/larger intrinsic phase speed. The positive correlation between GW amplitudes and zonal winds during solar minimum is thus unexpected at first glance, but may be explained by a downward shift of the GW maximum owing to thermal shrinking of the MLT wind systems. In such a case, GWs already maximize in the upper mesosphere. Then, strong/weak mesospheric easterlies, which are connected with weak/strong lower thermospheric westerlies, are connected with large/small GW amplitudes, large/small GW drag and consequently strong/weak westerly winds at greater altitudes. This may explain the positive correlation during solar minimum, while there is a negative correlation during the other years, then simply in accordance with linear theory.

Whether or not the above mentioned coupling processes really work requires more detailed analyses, including more satellite analyses, further radars, and numerical modeling. However, the observations of MLT GWs, mean winds, and reference heights already suggest that there is a height shift during solar minimum, which may influence vertical coupling between mesosphere and lower thermosphere. The recent solar minimum represents an extreme case, but the fundamental variability, as shown

by the LF measurements, was not qualitatively (although quantitatively) different from the last solar minimum, at least as far as the LF measurements at Collm are concerned. In the thermosphere, however, density decrease during the recent minimum was extreme. Thus, there are still open questions concerning solar variability and its effect on the MLT.

## Acknowledgements

This study was supported by DFG under grant JA 836/22-1.

## References

- Bremer, J., Peters, D., 2008: Influence of stratospheric ozone changes on long-term trends in the meso- and lower thermosphere. *J. Atmos. Sol.-Terr. Phys.*, 70, 1473–1481.
- Bremer, J., Hoffmann, P., Latteck, R., Singer, W., Zecha, M., 2009: Long-term changes of (polar) mesosphere summer echoes. *J. Atmos. Sol.-Terr. Phys.*, 71, 1571–1576.
- DeLand, M.T., Shettle, E.P., Thomas, G.E., Olivero, J.J., 2006: A quarter-century of satellite polar mesospheric cloud observations. *J. Atmos. Sol.-Terr. Phys.*, 68, 9–29.
- Emmert, J.T., Lean, J.L., Picone, J.M., 2010: Record-low thermospheric density during the 2008 solar minimum. *Geophys. Res. Lett.*, 37, L12102, doi:10.1029/2010GL043671.
- Fröhlich, K., Schmidt, T., Ern, M., Preusse, P., de la Torre, A., Wickert, W., Jacobi, Ch., 2007: The global distribution of gravity wave energy in the lower stratosphere derived from GPS data and gravity wave modelling: Attempt and challenges. *J. Atmos. Sol.-Terr. Phys.*, 69, 2238–2248.
- Gavrilov, N.M., Jacobi, Ch., Kürschner, D., 2001: Short-period variations of ionospheric drifts at Collm and their connection with the dynamics of the lower and middle atmosphere. *Phys. Chem. Earth*, 26, 459–464.
- Gray, L. J., Beer, J., Geller, M., Haigh, J. D., Lockwood, M., Matthes, K., Cubasch, U., Fleitmann, D., Harrison, G., Hood, L., Luterbacher, J., Meehl, G.A., Shindell, D., van Geel, B., White, W., 2010: Solar influences on climate. *Rev. Geophys.*, 48, RG4001, doi:10.1029/2009RG000282.
- Hocking, W.K., 2005: A new approach to momentum flux determinations using SKiYMET meteor radars. *Ann. Geophys.* 23, 2433–2439.
- Jacobi, Ch., Kürschner, D., 2006: Long-term trends of MLT region winds over Central Europe. *Phys. Chem. Earth*, 31, 16–21.
- Jacobi, Ch., Gavrilov, N.M., Kürschner, D., Fröhlich, K., 2006: Gravity wave climatology and trends in the mesosphere/lower thermosphere region deduced from low-frequency drift measurements 1984-2003 (52.1°N, 13.2°E). *J. Atmos. Sol. –Terr. Phys.*, 68, 1913–1923.
- Jacobi, Ch., Hoffmann, P., Kürschner, D., 2008: Trends in MLT region winds and planetary waves, Collm (52°N, 15°E). *Ann. Geophys.*, 26, 1221–1232.
- Jacobi, Ch., 2011: Meteor radar measurements of mean winds and tides over Collm (51.3°N, 13°E) - comparison with LF drift measurements 2005-2007. *Adv. Radio Sci.*, in print.

- Keuer, D., Hoffmann, P., Singer, W., Bremer, J., 2007: Long-term variations of the mesospheric wind field at mid-latitudes. *Ann. Geophys.*, 25, 1779–1790.
- Kodera, K., 1993: Quasi-decadal modulation of the influence of the equatorial quasi-biennial oscillation on the north polar stratospheric temperatures. *J. Geophys. Res.*, 98, 7245–7250.
- Kürschner, D., Schminder, R., Singer, W., Bremer, J., 1987: Ein neues Verfahren zur Realisierung absoluter Reflexionshöhenmessungen an Raumwellen amplitudenmodulierter Rundfunksender bei Schrägeinfall im Langwellenbereich als Hilfsmittel zur Ableitung von Windprofilen in der oberen Mesopausenregion. *Z. Meteorol.*, 37, 322–332.
- Kürschner, D., Jacobi, Ch., 2003: Quasi-biennial and decadal variability obtained from long-term measurements of nighttime radio wave reflection heights over central Europe. *Adv. Space Res.*, 32, 1701–1706.
- Mertens, C.J., Mlynczak, M.G., Lopez-Puertas, M., Wintersteiner, P.P., Picard, R.H., Winick, J.R., Gordley, L.L., Russell III, J.M., 2001: Retrieval of mesospheric and lower thermospheric kinetic temperature from measurements of CO<sub>2</sub> 15 μm earth limb emission under non-LTE conditions. *Geophys. Res. Lett.*, 28, 1391–1394.
- Ortiz de Adler, N., Elias, A. G., 2008: Latitudinal variation of foF2 hysteresis of solar cycles 20, 21 and 22 and its application to the analysis of long-term trends. *Ann. Geophys.*, 26, 1269–1273.
- Placke, M., Stober, G., Jacobi, Ch., 2010: Gravity wave momentum fluxes in the MLT—Part I: Seasonal variation at Collm (51.3°N, 13.0°E). *J. Atmos. Sol.–Terr. Phys.*, doi:10.1016/j.jastp.2010.07.012.
- Preusse, P., Ern, M., Eckermann, S. D., Warner, C. D., Picard, R. H., Knieling, P., Krebsbach, M., Russell, J. M., Mlynczak, M. G., Mertens, C. J., Riese, M., 2006: Tropopause to mesopause gravity waves in August: measurement and modelling. *J. Atmos. Sol.–Terr. Phys.*, 68, 1730–1751.
- Russell, J. M. III, Mlynczak, M. G., Gordley, L. L., Tansock, J., Esplin, R., 1999: An overview of the SABER experiment and preliminary calibration results. In: *Proceedings of the SPIE*, 3756, 44th Annual Meeting, Denver, Colorado, July 18–23, 277–288.
- Solomon, S. C., Woods, T. N., Didkovsky, L. V., Emmert, J. T., Qian, L., 2010: Anomalously low solar extreme-ultraviolet irradiance and thermospheric density during solar minimum. *Geophys. Res. Lett.*, 37, L16103, doi:10.1029/2010GL044468.
- Unglaub, C., Jacobi, Ch., Schmidtke, G., Nikutowski, B., Brunner, R., 2011: EUV-TEC proxy to describe ionospheric variability using satellite-borne solar EUV measurements: first results. *Adv. Space Res.*, 47, 1578–1584.
- Woods, T. N., Bailey, S., Eparvier, F., Lawrence, G., Lean, J., McClintock, B., Robie, R., Rottmann, G. J., Solomon, S. C., Tobiska, W. K., White, O. R., 2000: TIMED Solar EUV Experiment. *Phys. Chem. Earth (C)*, 25, 393–396.
- Woods, T. N., Francis, G. E., Bailey S. M., Chamberlin, P. C., Lean, J., Rottmann, G. J., Solomon, S. C., Tobiska, W. K., Woodraska, D. L., 2005: Solar EUV Experiment (SEE): Mission overview and first results. *J. Geophys. Res.*, 110, A01312, doi: 10.1029/2004JA010765.